# CHAPTER 4 RESULTS AND DISCUSSION

### 4.1 Characterization of ancient pottery

In this research, the ancient pottery from Nan was obtained from local archaeological authorities and Department of History, faculty of Humanities, Chiang Mai University. These sherd samples were discovered from different sources of Ja-Manas kiln site, Doi Fuang Moh kiln, Dong Poo Ho kiln and Nong Tom kiln, which were labeled as JQA.SH, FQB.SH, PQC.SH and NQD.SH, respectively.



**Figure 4.1** The typical photo of the samples (scale unit length: 1 cm).

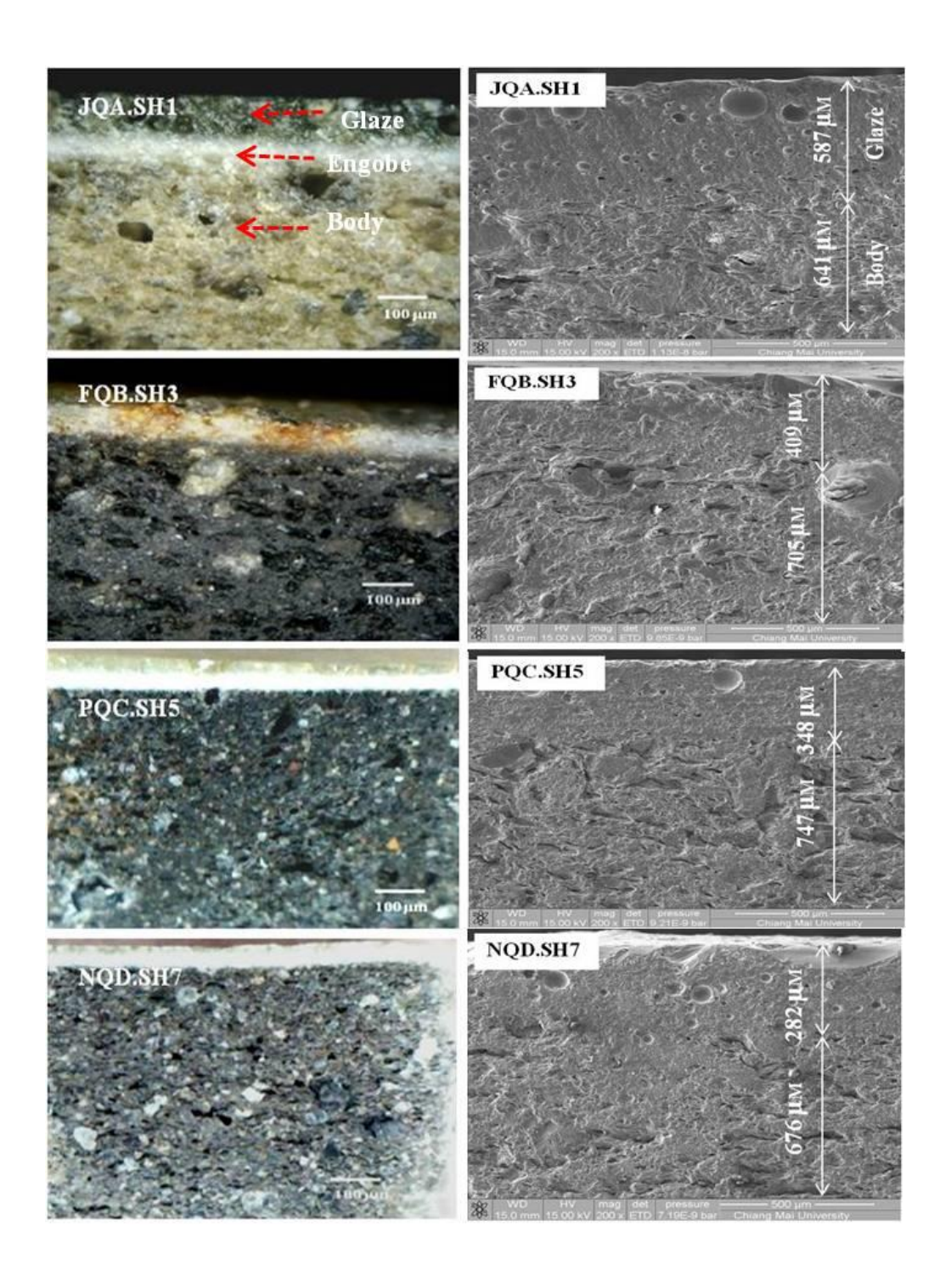


Figure 4.2 Decorative techniques: patterns with stripes, naturally [1].

The technology of ancient pottery could be explored by studying numerous vessels and fragments that have survived. The preserved pottery kilns, moulds, as well as pictures on the vases and written sources were considered as important sources of information in this respect. The products of the excavated kiln sites had dark stoneware body decorating, process of the dark color body categories: applying engobe coating layer of white fine clay on the green-body. There were two main categories of the pottery manufactured here, jar with single mouth-rim and jar with double mouth-rim, shallow bowls and plates of various sizes. Glaze was intentionally applied over thin layer of engobe on the interior leaving the exterior unglazed or covering with natural glaze. The green-glazed stoneware categories were found in the excavation kiln sites at JQA.SH1, FQB.SH3, PQC.SH5 and NQD.SH7. Another type of product that fell into unglazed group had high-fired stoneware body and decorative patterns with natural stripes. They were found in the excavation kiln sites at JQA.SH2, FQB.SH4, PQC.SH6 and NQD.SH8 (Table 4.1). Consistent with Usanee (2015) and Praicharnjit (2002), they said unglazed group has high-fired stoneware body and decorative patterns with natural stripes, combedwavy bands and impressed on shoulder-round (Figure 4.2). Analysis of sherds in cross-section using optical microscopy revealed the bodies had brown or black color. In addition, they were coarse-grained due to the presence of a high percentage of fine sand. This sand acted as grog in the body. The sample glazes were in the 200-500 µm thickness range. JQA.SH1 glaze showing a thin glaze layer and slip layer over the body were used between glaze and body (Figure 4.3). Generally, the formation of the middle layer was related to the chemical composition of both body and glaze, to the thickness of the glaze and to the control of firing temperature in firing process. In addition, during the firing process when heated to 1200 °C, the vitreous glaze infiltrates into the surface of the body, thus creating the middle layer. In the formation of the middle layer, the infiltration ratio of different elements in the vitreous glaze was different [78]. The samples from Ban Bo Suak kiln displayed glaze with more bubbles of different sizes (Figure 4.4).

 Table 4.1 The configurations of ancient sherds.

Sample	Site name	Label	Type	Description
No.				
1.	Ja-Manas	JQA.SH1	Glaze	Green glazed, coarse stoneware, small food bowls or plates.
2.	Ja-Manas	JQA.SH2	Unglazed	Unglazed stoneware, coarsegrained, single mouth-rim jars.
3.	Fuang Moh	FQB.SH3	Glaze	Green glazed stoneware body, coarse-grained hard and thin paste, small food or liquid containers.
4.	Fuang Moh	FQB.SH4	Slipped	Coarse-grained, external face with slipped.
5.	Dong Poo Ho	PQC.SH5	Glaze	Green glaze, stoneware ,coarse-grained, bowls or plates
6.	Dong Poo Ho	PQC.SH6	Unglazed	External face with slipped, small food or liquid containers
7.	Nong Tom	NQD.SH7	Glaze	Hard and thin paste, Green glazed, stoneware ,coarse-grained, thick paste (<1 cm)
8.	Nong Tom	NQD.SH8	Slipped	Coarse-grained, single mouth-rim, decoration representing cosmological,
				Unglazed stoneware



**Figure 4.3** The cross section of pottery sherds with layer structure in body and glaze showed dark stoneware bodies engobe decoration.

The effects in the samples were due to various factors: glaze gaseous matter was trapped because the glass was not fired at high enough temperature to liberate or dissolve it and should approach final temperature very slow. The bubbles were formed during the process of firing in the kiln. Specifically, when it reached a high temperature, the organic material in the glaze and body turned out from substances like CO, CO<sub>2</sub>, SO<sub>2</sub>, etc. A certain amount of gas which did not have time to escape would be stuck in the liquid glaze and eventually took the form of bubbles. Thus, the difference in diameter, amount and distribution of bubbles could reflect the difference in the material and manufacture technology. Moreover, the middle layer between the body and glaze could be clearly observed on all samples [79]. At 1100 °C top temperature, if interface sealed, gases escaped through unglazed areas [80]. As glaze melted, the firing rate should be slow or maturing temperature held to facilitate clearing of bubbles etc. Some vessels broke during firing due to too rapid heating or cooling or imperfection in the pottery. Vessels might also blister and warp, forming distorted sherds or wasters that were easily recognizable in the archaeological record and were often found in the vicinity of firing areas.

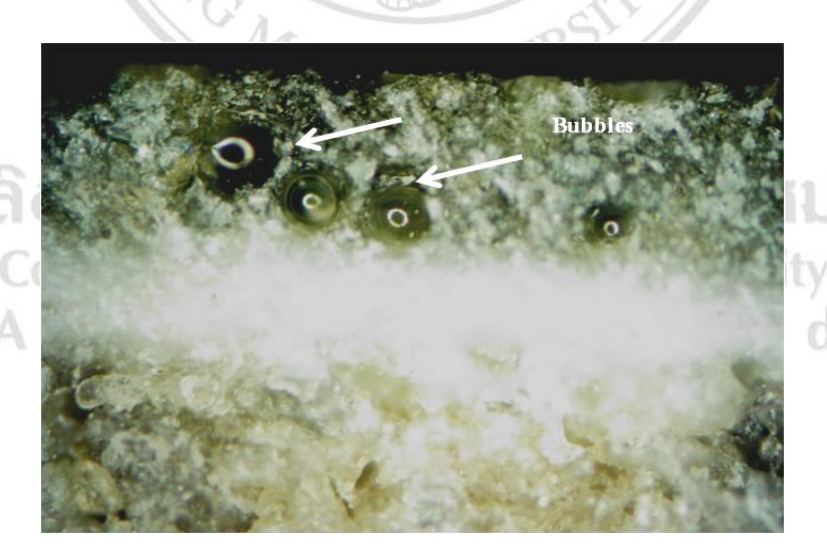


**Figure 4.4** The sherd samples have shown a glaze which is full of bubbles.

By examining the mineralogical structure of a fired vessel, it could be estimated that the firing condition, included temperature, duration and atmosphere. In addition, surface color might vary in a single pot, if some areas of the firing or facility were exposed to greater oxygen than others. Firing atmosphere could be controlled by potters in a number of ways. Black or dark-brown vessels were typically produced in a reducing atmosphere. In their oxygen-poor atmosphere, the carbon in the vessel body was not lost and carbon from fuels might be deposited on the vessel surface, producing a pot that was dark in color. Vessel color might be differing from the core to the surface depending on the firing and cooling condition and the degree to which organic materials were fully oxidized. Firing temperatures contributed to the identification of firing, whether vessels were fired in open pits or enclosed ovens or kilns [81]. Surface and core color could provide information about the firing atmosphere, whether oxygen rich (oxidizing) in which case carbonaceous minerals will be fully burnt and the vessel would be light in color, or oxygen poor (reducing) which would produce blackened vessels [82]. The core colors would also provide information on cooling after firing [83]. Chemically, most clay was composed of a small number of elements and compounds, mainly silicates, aluminum and water joined in a crystalline structure [84]. Other element, including potassium, sodium, calcium, and iron, among others, occur in smaller quantities (Figure 4.5). The sinter process was usually accompanied by other changes within the material such as chemical composition and crystal structure, distribution of pore size, crack and shape in which some were undesirable (Figure 4.6).

> Copyright<sup>©</sup> by Chiang Mai University All rights reserved

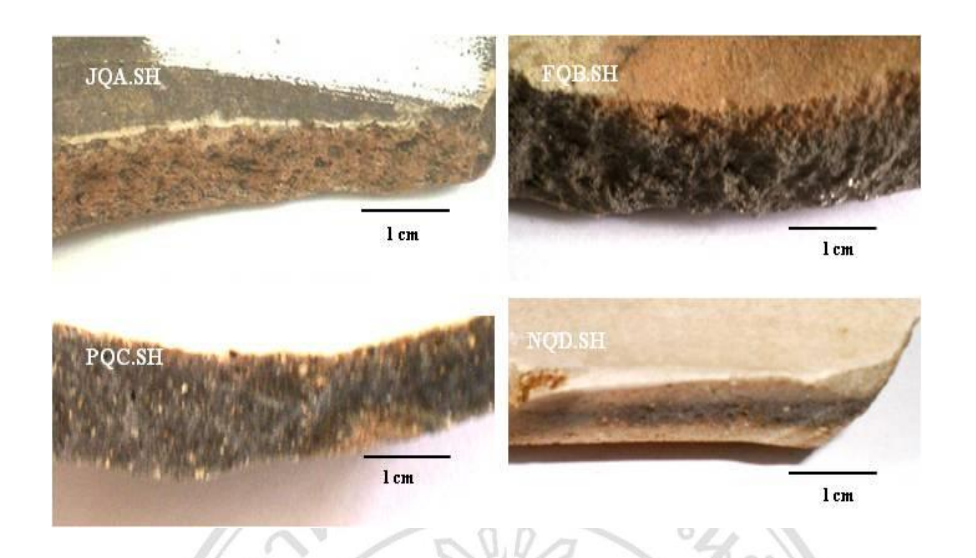


Figure 4.5 The carbon coke effect on the pottery sherds.

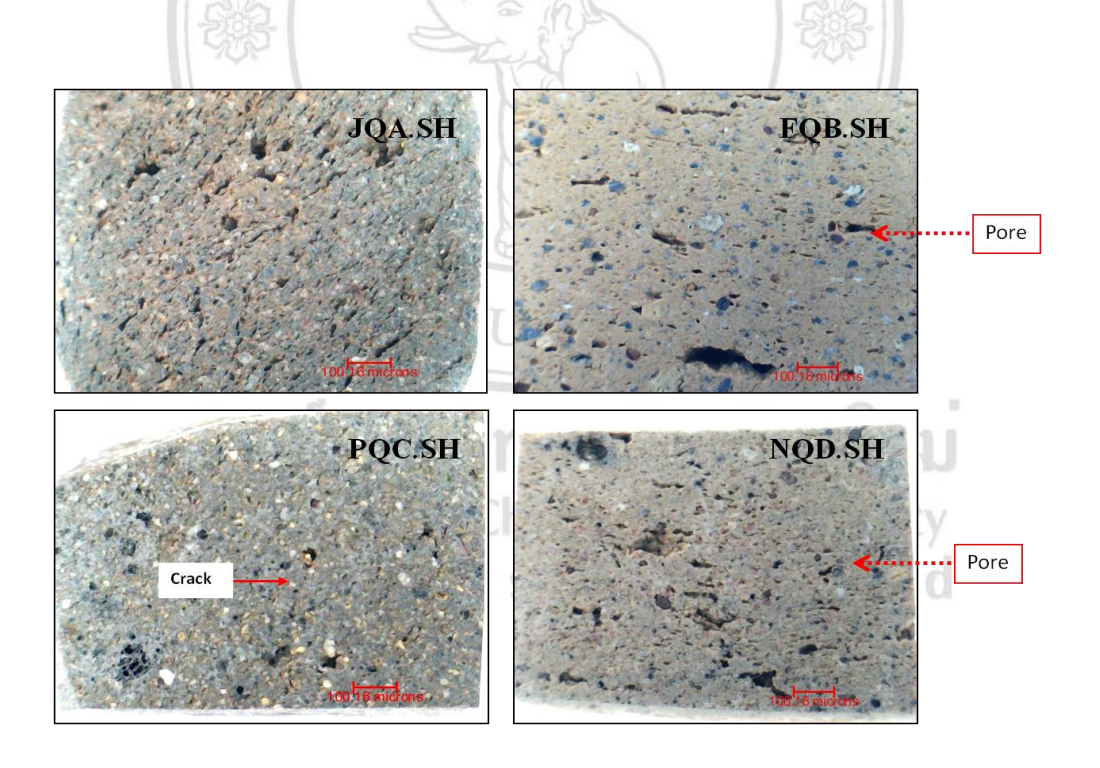


Figure 4.6 Cross section in samples showed pores and cracks in the body.

The chemical compositions of all samples were analyzed by X-Ray Fluorescence analysis as shown in Table 4.2. The main chemical composition of sherds was SiO<sub>2</sub> > 71 wt. %. The samples of glaze group; JQA.SH1, FQB.SH3, PQC.SH5 and NQD.SH7 had highest amount of Fe<sub>2</sub>O<sub>3</sub>, while, unglaze group JQA.SH2, FQB.SH4, PQC.SH6 and NQD.SH8 were less than the glaze group, the features of chemical compositions of all samples were identified using chemical analysis and mineralogical were similar to the local clay near the kiln sites. The first step of ceramic manufacture was to acquire the necessary raw materials and prepare the clay. Potters typically obtained their raw materials from sources close to home, usually 1-6 kilometers from the manufacturing site [85]. The samples JQA.SH1, FQB.SH3, PQC.SH5 and NQD.SH7 which were analyzed by XRD, showed that phase structure was quartz; tridymite and mullite phase (Figure 4.7).

Table 4.2 Chemical analysis of sherds obtained from Ban Bo Suak.

T 477 11

	10.1	100			A A / I				111		
Compound		,				11		2			
(wt.%)	$SiO_2$	Al <sub>2</sub> O <sub>3</sub>	K <sub>2</sub> O	Na <sub>2</sub> O	Fe <sub>2</sub> O <sub>3</sub>	TiO <sub>2</sub>	CaO	MgO	MnO	$ZrO_2$	$P_2O_5$
JQA.SH1	76.69	10.82	2.62	AI I	6.97	1.72	1.00	-	-	0.20	-
JQA.SH2	71.76	12.99	2.04	0.08	7.14	1.54	2.59	0.39	0.25	0.10	0.30
FQB.SH3	71.02	14.37	2.34	11-5	8.92	2.04	1.16	O-B	lhi	0.18	-
FQB.SH4	75.30	12.08	1.37	0.03	4.41	1.31	3.49	0.42	0.15	0.11	0.52
PQC.SH5	73.21	10.80	2.66	h t	9.09	1.61	2.25	r- V	0.21	0.19	-
PQC.SH6	72.39	15.42	1.55	0.03	7.28	1.63	0.75	0.24	0.08	0.12	0.11
NQD.SH7	71.35	11.54	2.55	-	10.48	1.59	2.21	-	0.15	0.16	-
NQD.SH8	71.52	14.18	3.36	-	7.19	2.22	2.75	-	0.10	0.22	0.11

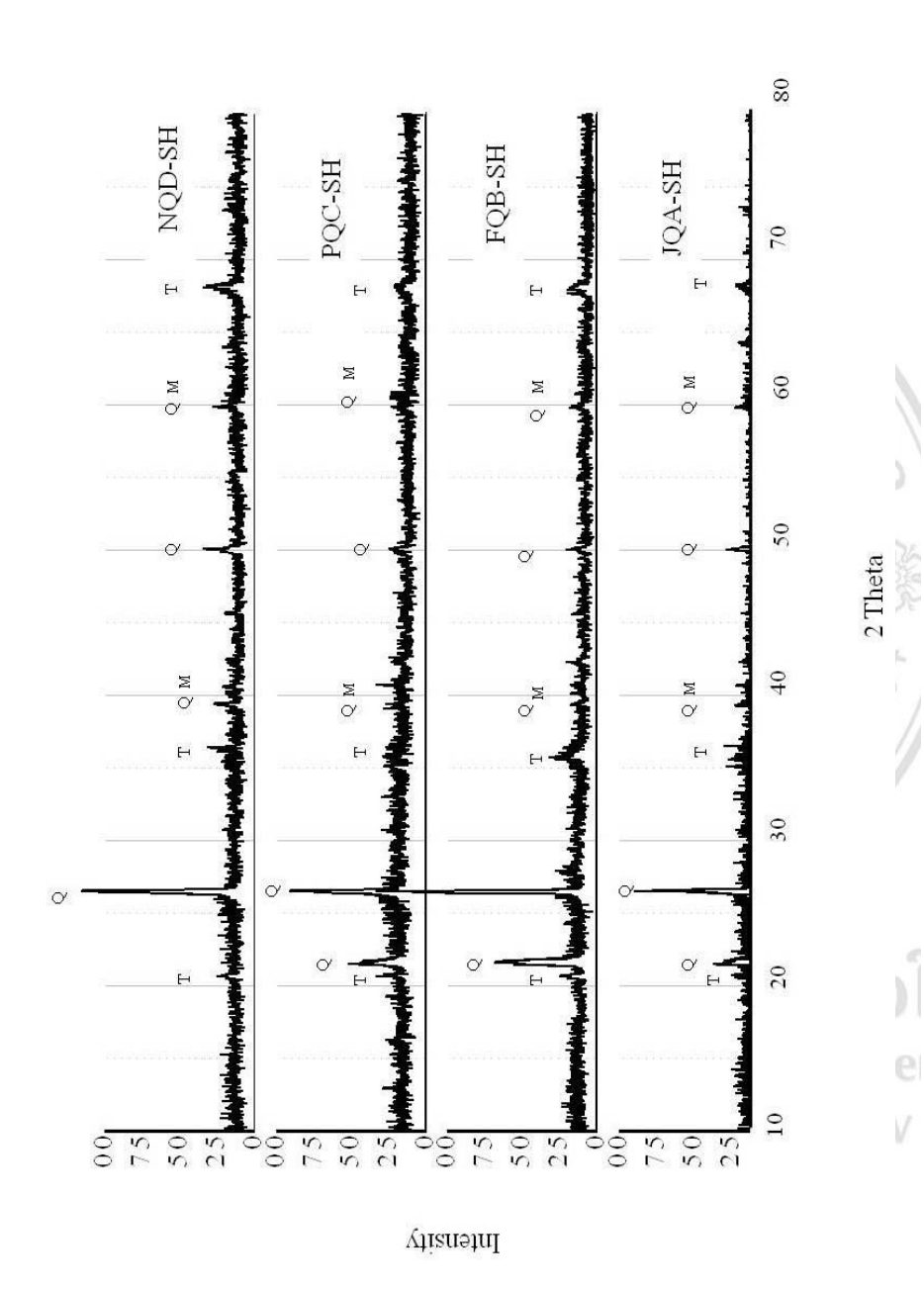


Figure 4.7 XRD patterns of the ancient Ban Bo Suak pottery sherds.

Q: Quartz, T: Tridymite and M: Mullite

NQD.SH had higher densification than PQC.SH and tridymite phase was decreased. The highest of densification was obtained in JQA.SH and FQB.SH. Besides, primary mullite phase was investigated. Thus, it was confirmed that JQA.SH and FQB.SH sherds were fired at high temperature of more than 1100 °C. However, mullite phase had not indicated in XRD patterns in Figure 4.7 because the mullite was transformed from meta-kaolinite that was slightly observed in these sherds. Mullite phase first appeared at the temperature around 1100 °C, its amount increased with the increase of temperature [86]. The amorphous SiO2 changed to cristobalite at above 1200 °C. It was confirmed that sherds were fired at high temperature of more than 1100 °C at temperature mullite grains were formed. It was likely shreds were fired at temperatures greater than 1000 °C since quartz were high content. This was also supported by the good correlation found among all sample. Variations in production techniques and vessels of ancient pottery should be viewed as had been conditioned in part by the quality and nature of the raw materials. Types of clays were distinguished by their mineral composition and the patterns of arrangement of their various mineral constituents and many kinds of clays had been defined. Most were constructed of layered crystalline sheets and included both two and three-layer of clays. Two- layer clays include kaolinites, a very common clay mineral that in its purest form was used in the manufacture of porcelain vessels. Three-layered clays included smectites and illite, frequently used by potters as paints or for decorative coating (slips) on vessel surfaces [87]. In addition, each of these clays responded somewhat differently to heat, resulting in variations in vessel color strength, shrinkage and in the temperatures required during firing. They also achieved a good knowledge on clay properties to select the raw materials, using a mixture of local clay resources, the red clays with the addition of grit for forming of clays, creating a specialized production of ceramic pieces [88].

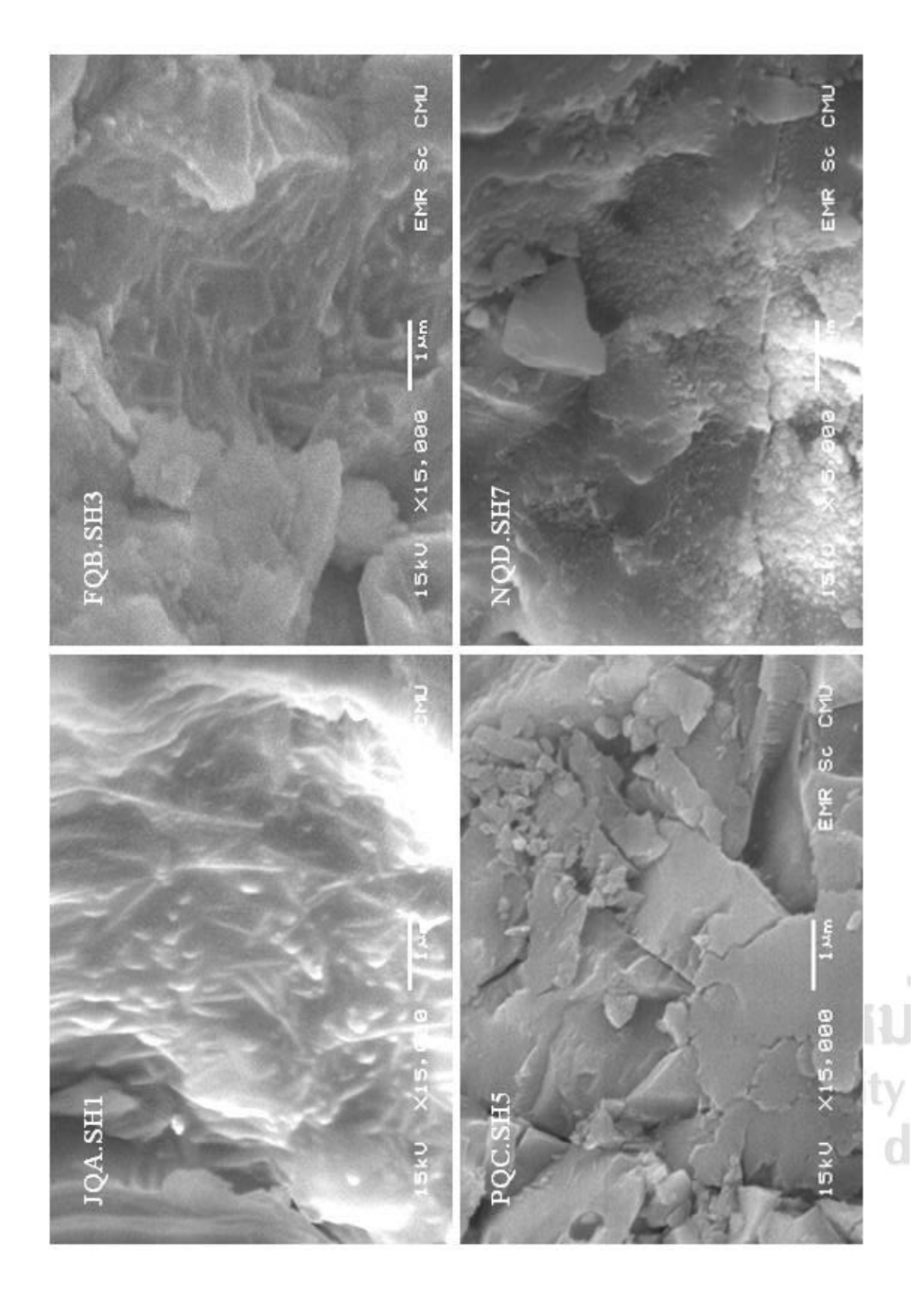


Figure 4.8 SEM micrographs of pottery sherds

The technology of ancient pottery was explored by the study from the numerous vessels and fragments that were discovered. Archaeological data of Nan ancient pottery showed preliminary results on the provenance and possible of mineralogy and clay chemistry of ancient pottery and local clay deposits. The results showed that these cultures had continuity in the ceramic tradition and a well-known usage of their natural resources. They also achieved a good knowledge on clay properties to select the raw materials, using a mixture of local clay resources, the red clays with the addition of grit for forming of clays, creating a specialized production of ceramic pieces. The products of the excavated kiln sites had dark stoneware body decorating process of the dark color body categories: applying used glaze coating on the green-body. The type of product that was unglazed had high fired stoneware body and decorative patterns with stripes and naturally. Main chemical composition of samples was quartz. The samples of glazed group had highest content of iron oxide, while unglazed group had content of iron oxide less than the glazed group. According to analysis of sherds in cross-section using optical microscopy revealed that the body was brown or black. In addition, they were coarse-grained due to high percentage of sand. The feature of chemical compositions of all samples was identified using chemical analysis and mineralogical were similar to the local clay near the kiln sites. The sample which were analyzed by XRD, showed that phase structure was quartz, tridymite and mullite phase. Mullite phase first appeared at the temperature around 1100 °C, its amount increased with the increase of temperature. A suitable combination of analytical techniques used for the research of ceramics provided useful information. It helps to explain the nature of the raw materials used in the manufacture, possible origin, production, or firing technology [89].

#### 4.2 Characterization of Ban Bo Suak Clays

The chemical composition of different Nan clays used in the investigation were shown in Table 4.3. The main chemical compositions of the clays was SiO<sub>2</sub> which was more than 80 wt.%. The oxides of alkaline and alkaline earth was lower

than 1 wt. %. However, the degree of iron oxide Fe<sub>2</sub>O<sub>3</sub> content of clays was high >1.6 wt. %, which played important role in the red-dark tone color of the ceramic after firing process [90]. Besides, it was found that the chemical composition of the clay samples after fired at 110°C was slightly decreased due to the diffusion into the environment. XRD patterns of these powder clays were presented in (Figure 4.9). It was indicated that quartz was the majority of phase in these powder clays, while some phase of kaolinite were investigated slightly. XRD patterns of samples indicated the main minerals were quartz, kaolinite, while small peak of microcline phase was observed in JQA clay (Figure 4.10).

The shapes and sizes of the powder clay particles were important for ceramic process, so it should be sieved to eliminate the large particle size and the residue from the clay materials. The different particle sizes of clays were separated by sieve analysis process, as shown in Table 4.4. It was found that the residue volume of FQB, NQD and JQA clays were about 57.98 wt.%, 56.29 wt.% and 54.73 wt.%, respectively. The minimum residue volume 45.38 wt. % was obtained for PQC clay. After sieve analysis, the average particle size (D (4,3)) of all clays were measured by laser diffraction technique. The average particle size of JQA, FQB, NQD and PQC were about 11.48  $\mu$ m, 9.63  $\mu$ m, 8.21  $\mu$ m and 7.96  $\mu$ m, respectively (Figure 4.11). It had a polygon shape and the particle sizes of all clays were less than 200  $\mu$ m.

ลิขสิทธิ์มหาวิทยาลัยเชียงใหม่ Copyright<sup>©</sup> by Chiang Mai University All rights reserved

**Table 4.3** Chemical analysis of powder clays unfired and after fired 1250 °C.

	Chemical analysis of clays (% wt.)								
Clay samples	SiO <sub>2</sub>	Al <sub>2</sub> O <sub>3</sub>	K <sub>2</sub> O	CaO	ZrO <sub>2</sub>	Fe <sub>2</sub> O <sub>3</sub>	MnO	TiO <sub>2</sub>	LOI
Unfired									
clay									
JQA	84.02	11.45	0.75	0.34	0.07	2.44	0.10	0.80	-
FQB	88.78	8.26	0.43	0.13	0.06	1.65	0.00	0.65	-
PQC	81.09	13.90	0.89	0.53	0.06	2.63	0.07	0.79	-
NQD	86.46	10.35	0.46	0.24	0.07	1.70	0.00	0.64	-
Fired clay	90	5	0	7			932		
JQA.F	87.51	10.33	0.67	<0.01	< 0.01	1.46	0.00	< 0.01	4.07
FQB.F	87.89	10.47	<0.01	0.00	< 0.01	1.63	0.00	< 0.01	3.99
PQC.F	80.48	16.67	0.81	<0.01	0.00	1.79	0.00	0.23	4.19
NQD.F	85.27	13.15	0.22	0.00	<0.01	1.357	0.00	< 0.01	3.22

Copyright<sup>©</sup> by Chiang Mai University All rights reserved

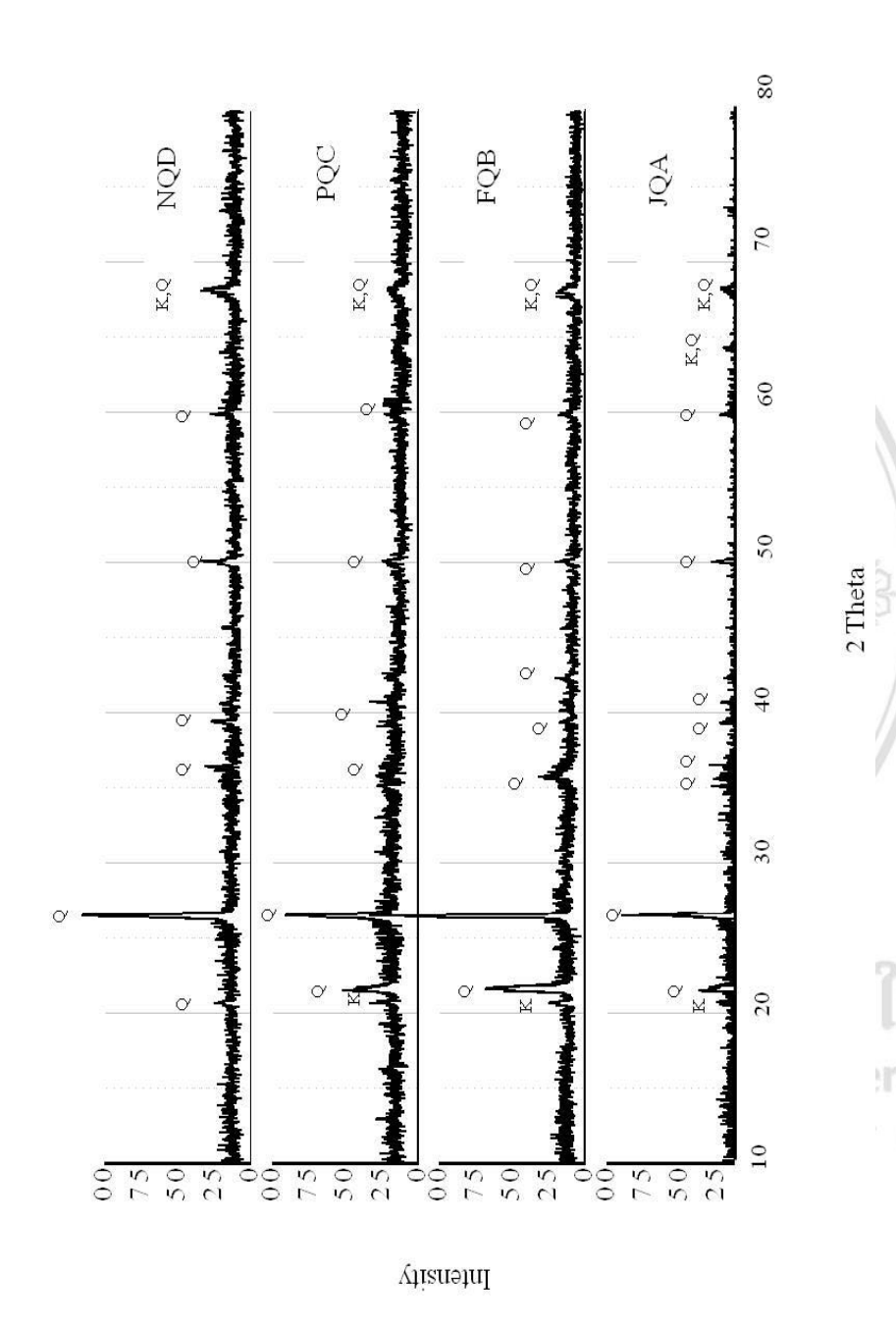
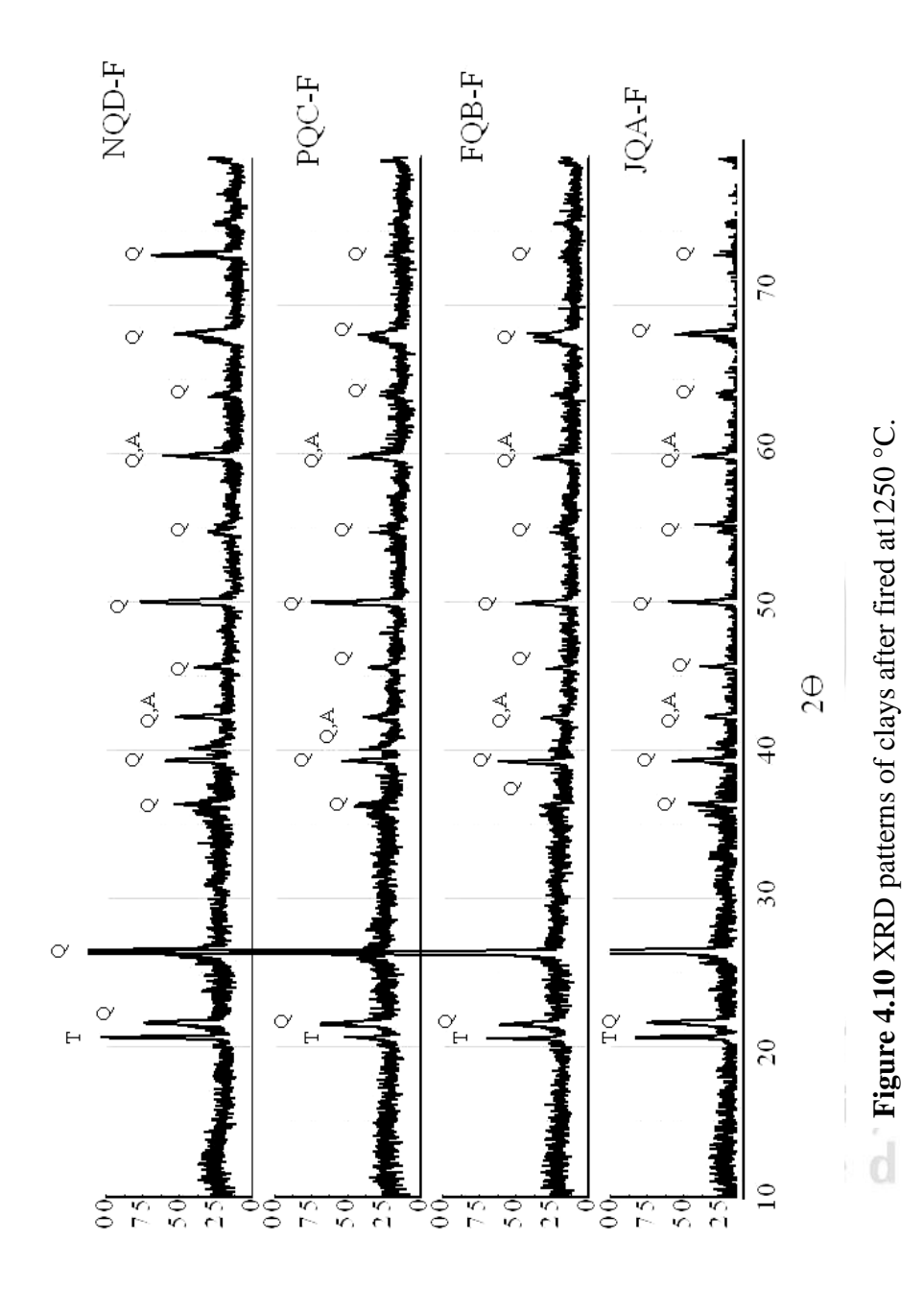


Figure 4.9 XRD patterns of the different powder clays from Ban Bo Suak.

Q = Quartz, K = kaolin



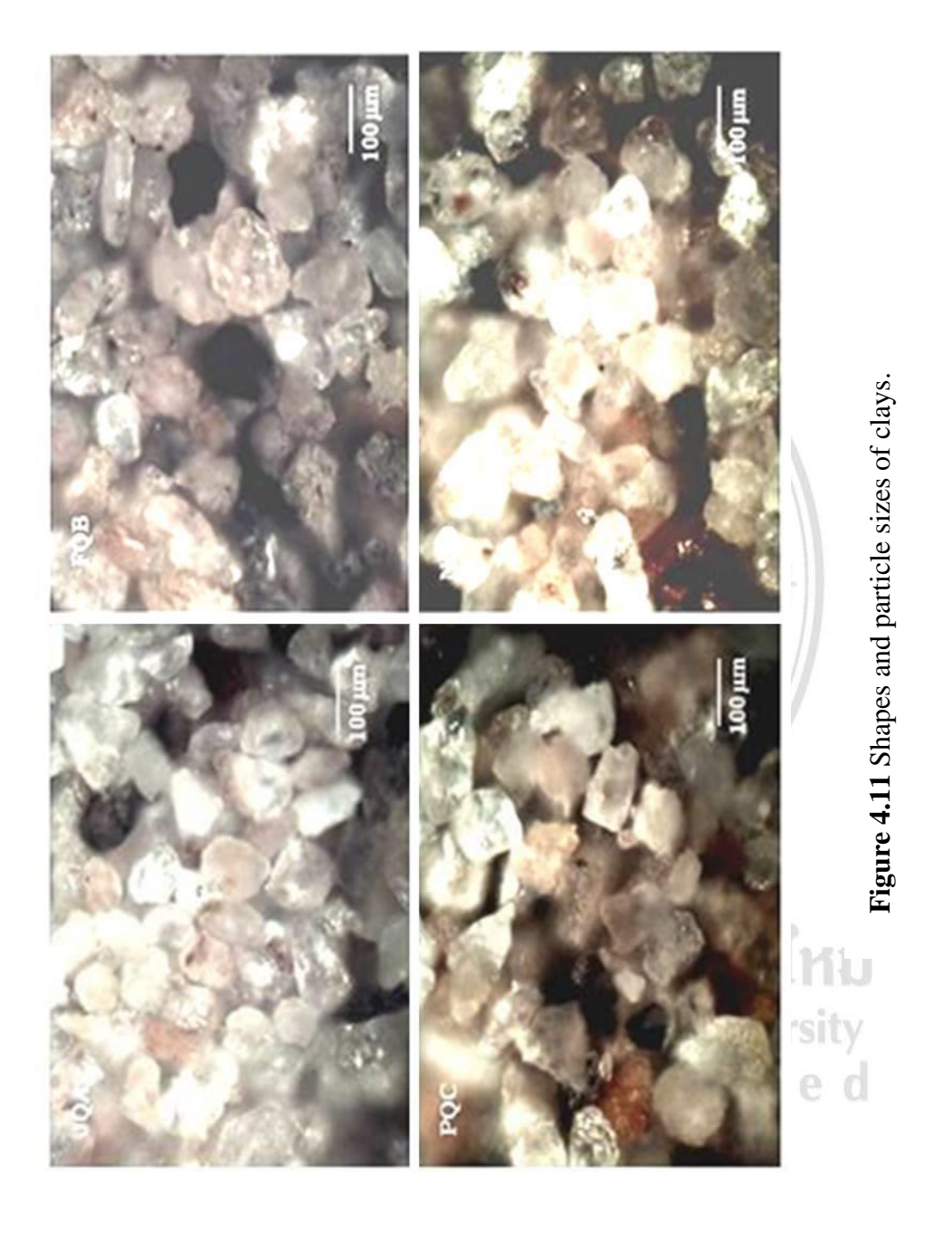
Q = Quartz, T = Tridymite and A = Anorthite

Intensity

Table 4.4 Sieve analysis and particle size of different clays

	Clay samples (%wt)				
Sieve (Mesh)	JQA	FQB	PQC	NQD	
60	23.84	10.09	9.41	13.94	
120	18.19	27.36	19.05	21.47	
200	9.27	11.05	9.32	11.67	
325	3.48	9.48	7.60	9.21	
Total (Quantity of residue remained on the siev	54.73 ve)	57.98	45.38	56.29	
Total (Quantity of clay)	45.22	42.02	54.62	43.71	
Particle size D [4,3]	11.48	9.63	7.96	8.21	

ลิขสิทธิ์มหาวิทยาลัยเชียงใหม่ Copyright<sup>©</sup> by Chiang Mai University All rights reserved



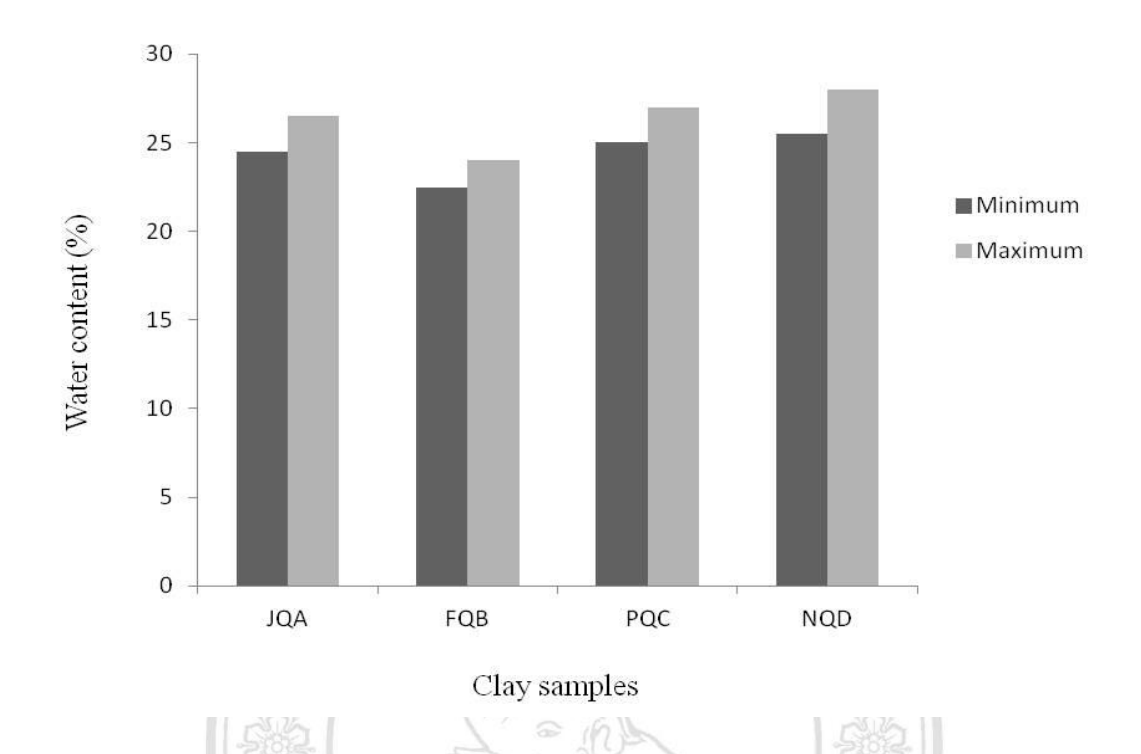


Figure 4.12 Percentage of water to cause toughness

Table 4.5 Percentage of water content

Percentage of water content							
Clay samples	Water co		Plasticity Index				
Allri	g min t s	max 🦲 S	erved				
JQA	24.5	27.0	2.0				
FQB	23.0	24.0	1.0				
PQC	25.0	27.0	2.0				
NQD	25.5	28.5	2.5				

 Table 4.6 Plasticity of clays with water solution for forming process

Clay samples	Plasticity	Forming	Color of
			fired clay
JQA	plastic	good	Brown
FQB	low plastic	weak	Orange-Brown
PQC	plastic	good	Brown
NQD	plastic	good	Brown
	1		
20%		22%	24%
26%		28%	30%
AII	right	s re	served

Figure 4.13 Plasticity of clays with water solution for forming process

Table 4.5 and 4.6 showed the powder clays were mixed with water content in forming process. It was found that JQA, PQC and NQD had 23-28.5 wt. %, respectively. While, FQB had the lowest water content of 23-24.0 wt. % because of the large particle size and high amount of free silica. Factors influencing plasticity might be related to the clay itself or to the forming process. Clay related factors were moisture content, mineralogical composition, particle size distribution, type of exchangeable cations, presence of salts and organic material. When water was added to dry clay, the first effect was an increase in cohesion, which tended to reach the maximum when water had nearly displaced all air from the pores between the particles. Addition of water into the pores induced the formation of a fairly high yield-strength body that, however, might crack or rupture readily on deformation [34].

ลิขสิทธิ์มหาวิทยาลัยเชียงใหม่ Copyright<sup>©</sup> by Chiang Mai University All rights reserved



Figure 4.14 The color of fired clay at different temperatures

#### 4.2.1 The color of clay samples

The samples were fired at different temperatures in the range of 800-1250 °C (Figure 4.14). It was found that after firing at 800-1000°C, clays turned light brown in color, but tended to be darker when it was fired at 1200-1250 °C. All clays had red-brown tone color due to high  $Fe_2O_3$  in the composition.

## 4.2.2 Water absorption

During drying at 110°C, H<sub>2</sub>O molecules between clays particles were volatized from surface of the clay so the particles were moved closer together, leading to the shrinkage of samples. However, the last positions of the H<sub>2</sub>O molecules became space or pores in clay body. This was confirmed from the high water absorption for the dried clays. Water absorption after fired at 1250°C was about 7.48 %, 6.55%, 8.01% and 7.18, respectively (Figure 4.15).

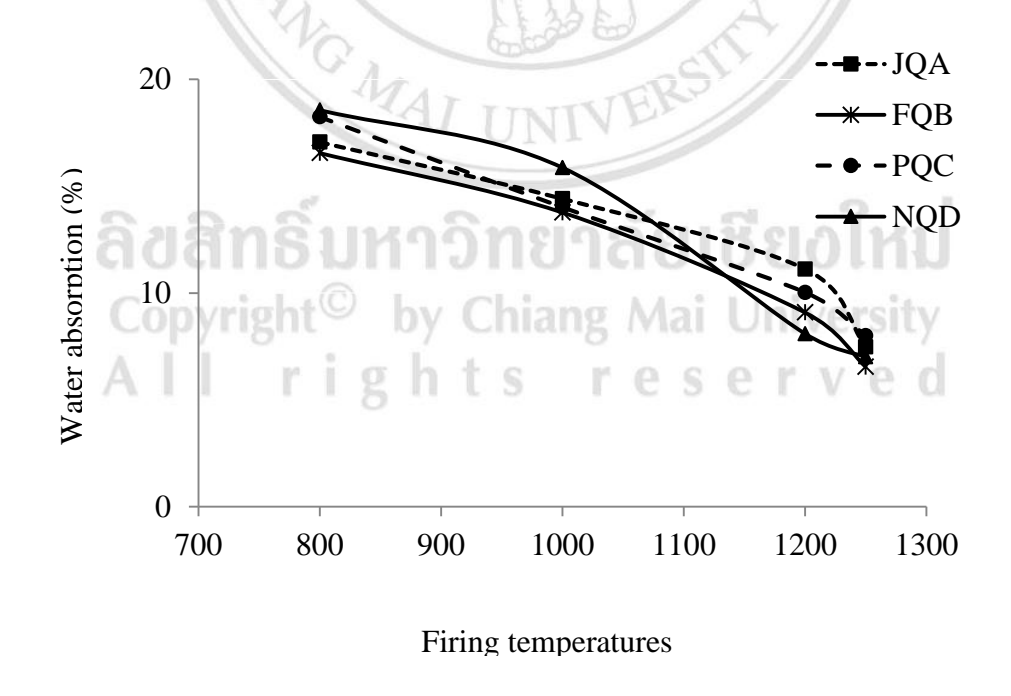


**Figure 4.15** The water absorption values of the fired clays at different temperatures

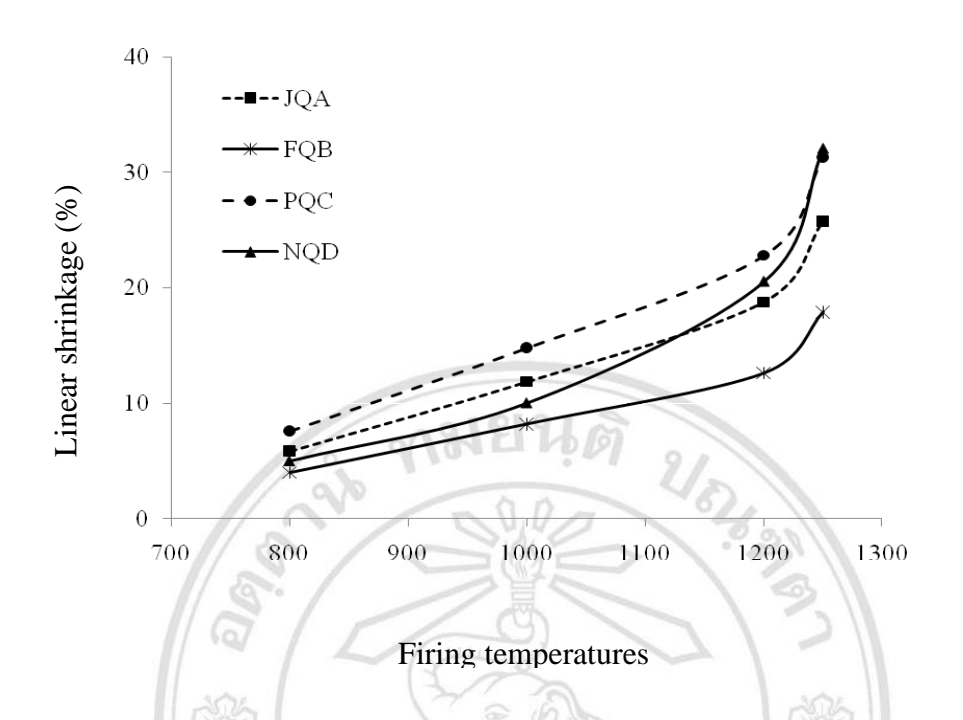


Figure 4.16 The firing shrinkage values of the fired clays at different temperatures

#### 4.2.3 Linear shrinkage

The highest drying shrinkage was obtained for PQC clay due to the smallest average particle size. After firing at 800-1250°C, the linear shrinkage value of all samples was significantly increased with higher firing temperature. However, the linear shrinkage values of the clay samples were obviously increased after fired at 1250 °C, which related directly to the lower water absorption. Linear shrinkage values of the JQA, FQB, PQC and NQD clays after fired at 1250°C were about 32.11 %, 30.41%, 37.10% and 34.65%, respectively (Figure 4.16). Moreover, the linear shrinkage of the different clays increased with an increase of Fe<sub>2</sub>O<sub>3</sub> content, which presented the fluxing effect. In pottery design, shrinkage value was essential fundamental for the calculated size of green sample because it was shrunk after firing process.

#### 4.2.4 Bending strength

Modulus of rupture (MOR) or bending strength values of the fired clays at different temperatures shown in Figure 4.17. Bending strength of all clays tended to be improved with an increase of firing temperature because of the elimination of porosity during vitrification process. The maximum strength was thus obtained in the fired clays at 1250°C. It was found that the bending strength after fired JQA, FQB, PQC and NQD were about 28.87, 23.94, 27.35 and 31.12 MPa, respectively. Bending strength of the fired ceramics could be implied to the various factors such as, degree of vitrification, mullite needle inter locking, grain size of the minerals glassy phase and residual quartz content as well as defects occurred in the body [91].

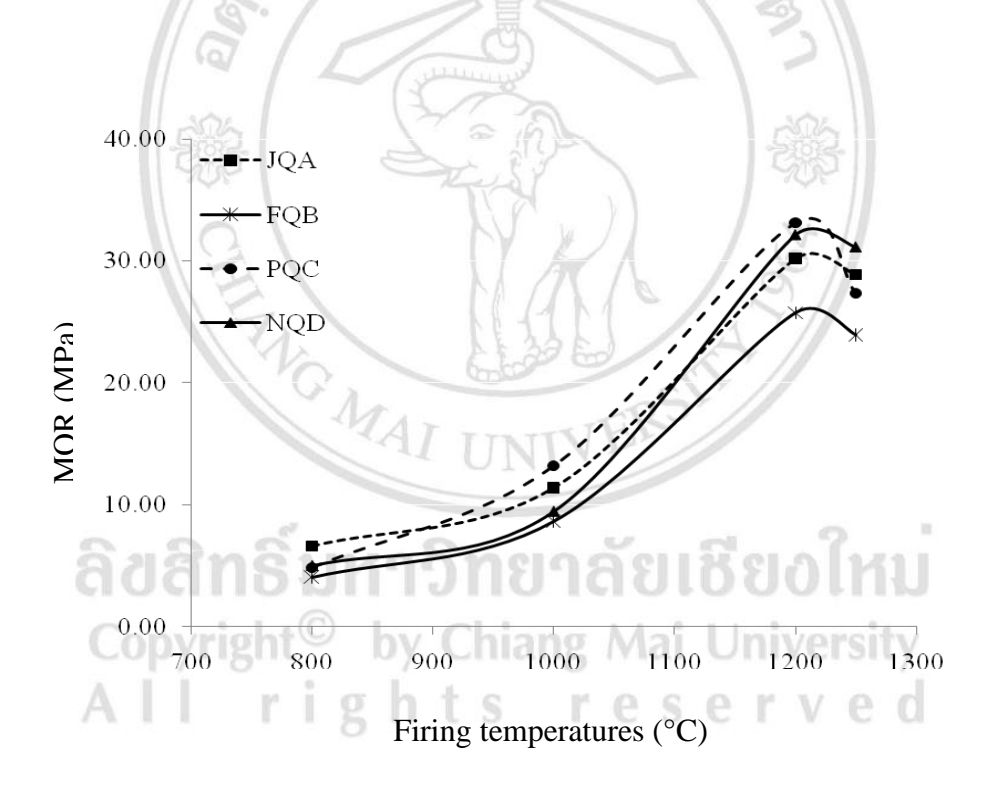


**Figure 4.17** Bending strength of the fired clays at different temperatures

#### 4.2.5 SEM micrographs

SEM micrographs of fired clays at 800 °C are shown in Figure 4.18. Much porosity was observed in all clays after being fired at 1000°C as shown in Figure 4.19. At 1200°C, the porosity was slightly decreased due to higher surface energy during vitrification, while the primary mullite phase was appeared (Figure 4.20). These primary mullite phases were developed from metakaolin after being fired at 1200°C [89]. Finally, the primary mullite was transformed into the secondary mullite after being fired above 1250°C, which was observed to confirm this behavior in Figure 4.21.

#### 4.2.6 Softening point

The softening point of the clays was measured by consideration of the flexural distance of the bar shape. It was found that all clays were stable without bending effect when it was fired up to 1280 °C. The softening points of these clays were less than 0.10 mm. In addition, FQB clay contained a higher content of quartz, which affected on the high resistant for warping defect in three clays sources (Figure 4.22). This was confirmed that Ban Bo Suak clays could be fired with glaze at high temperatures (< 1280 °C).

ลิขสิทธิ์มหาวิทยาลัยเชียงใหม Copyright<sup>©</sup> by Chiang Mai University All rights reserved

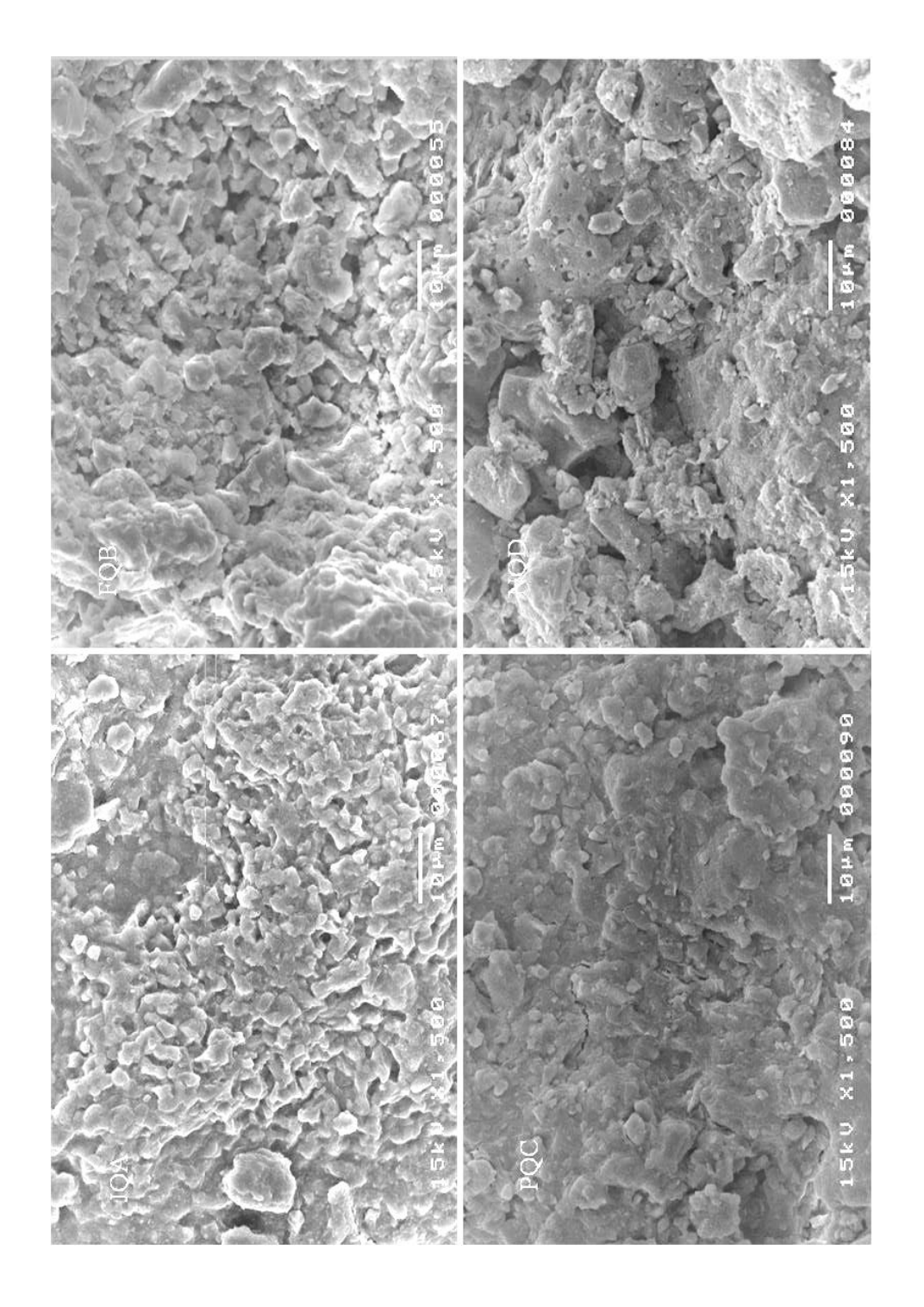


Figure 4.18 SEM micrographs of clays being fired at 800 °C

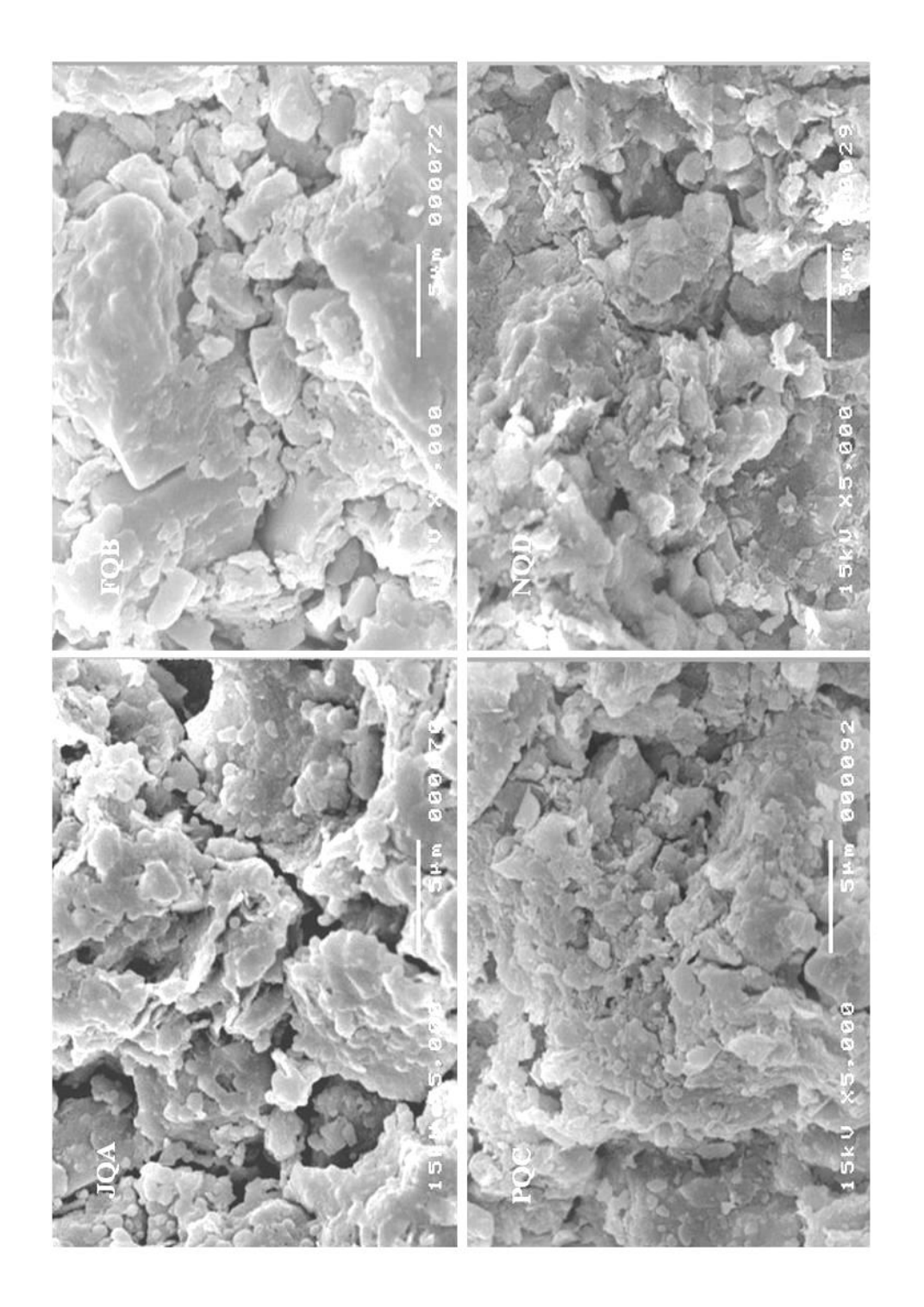


Figure 4.19 SEM micrographs of clays being fired at 1000 °C

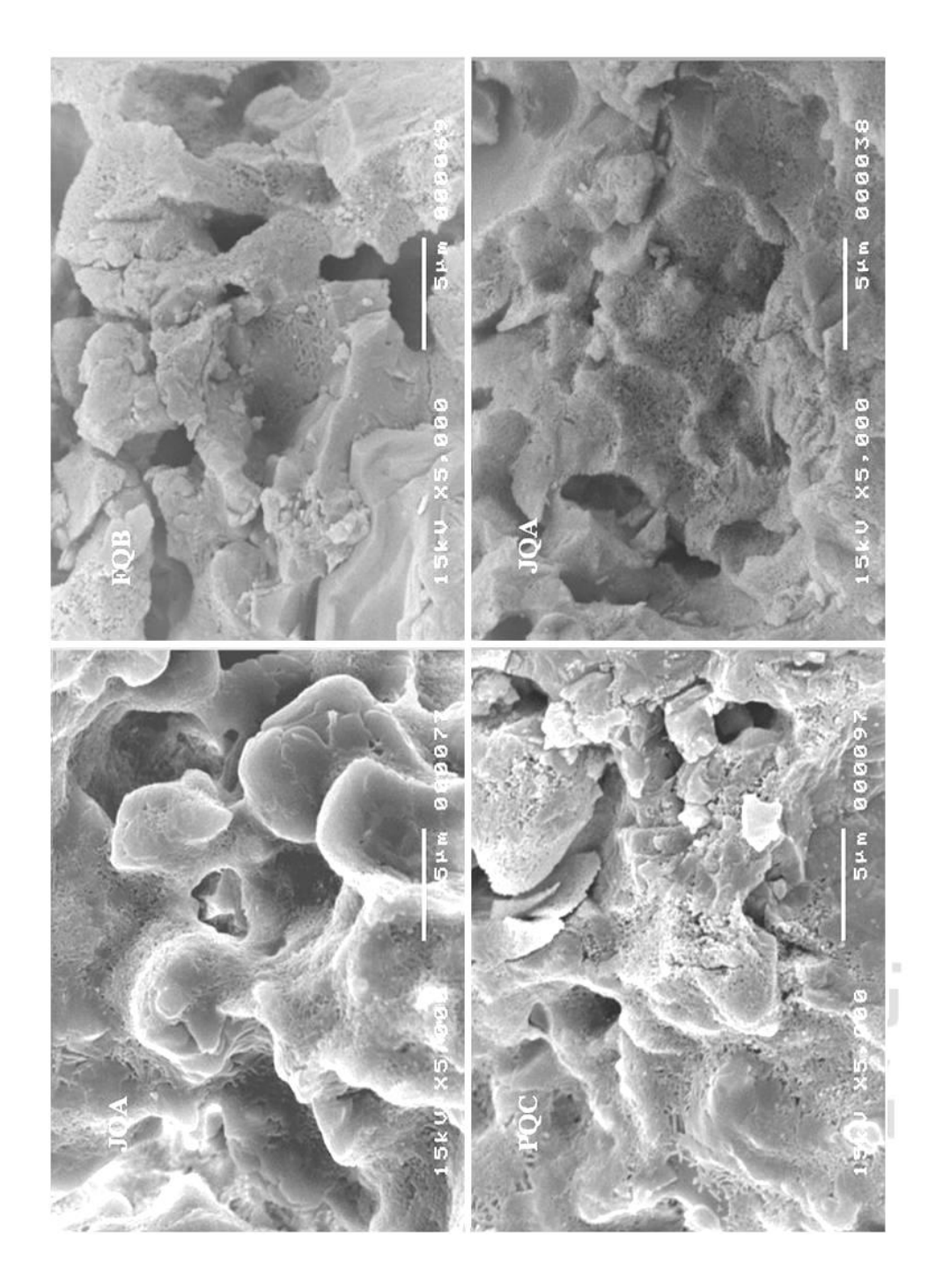


Figure 4.20 SEM micrographs of clays being fired at 1200 °C

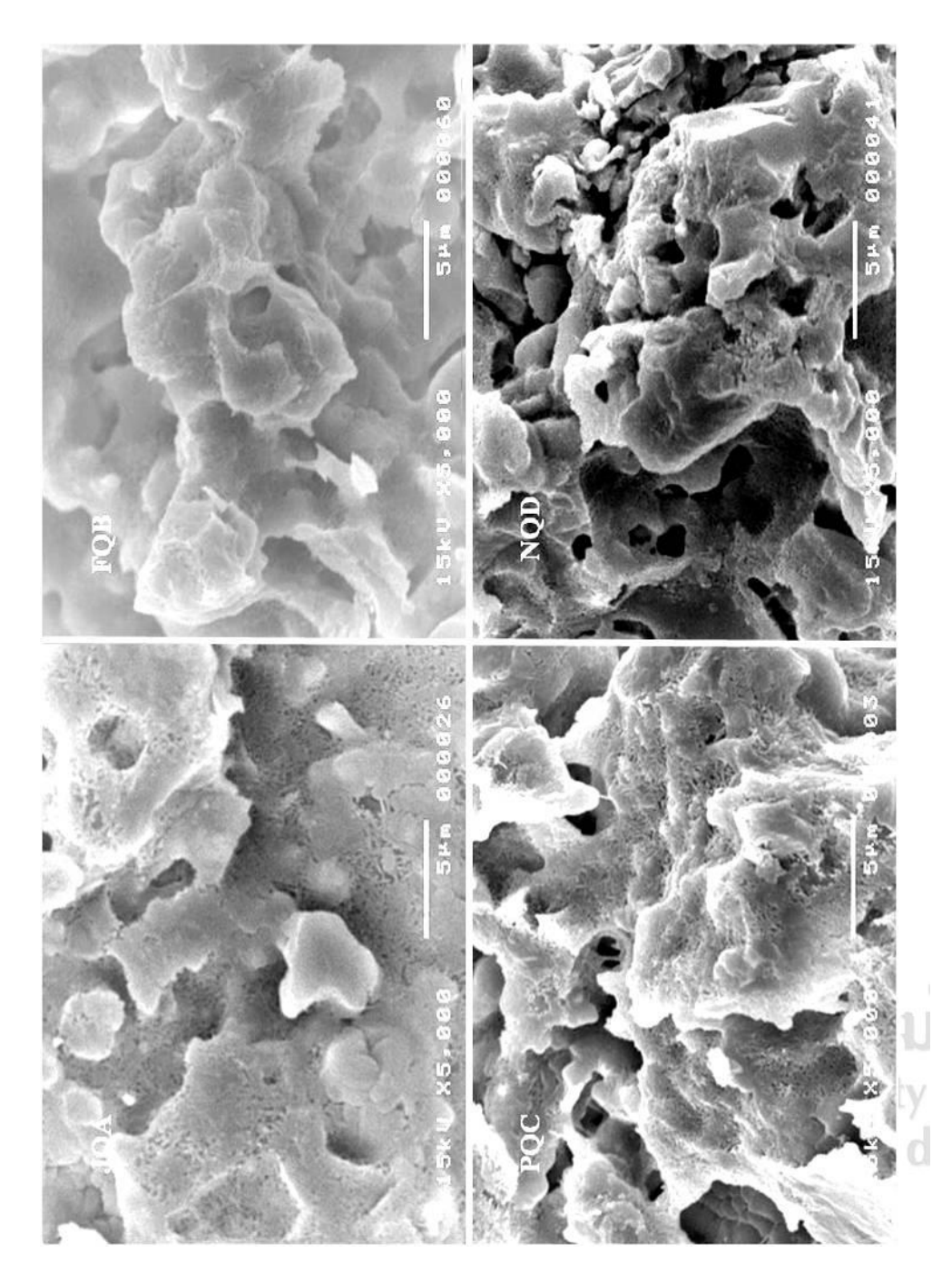


Figure 4.21 SEM micrographs of clays being fired at 1250  $^{\circ}\mathrm{C}$ 

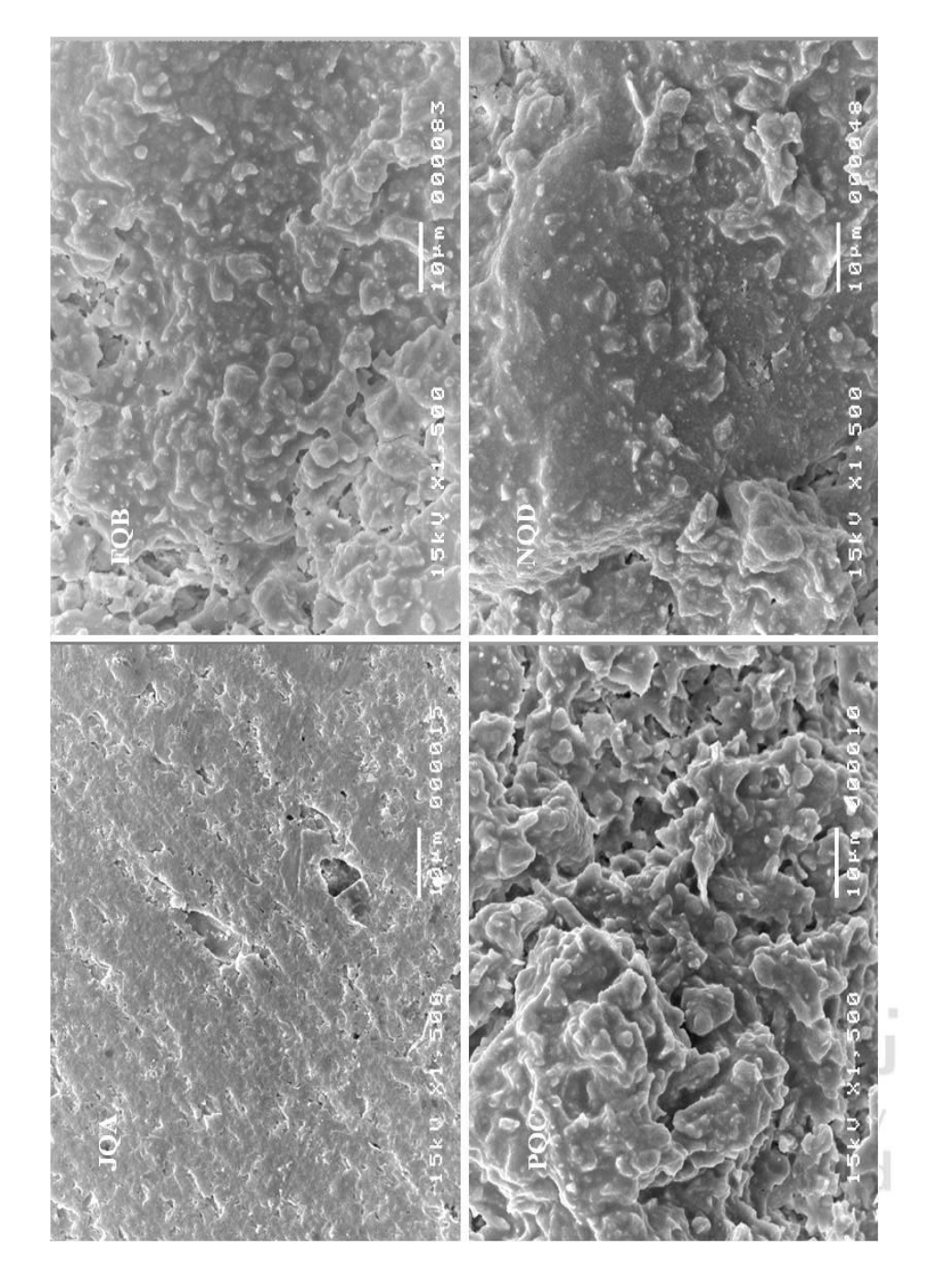


Figure 4.22 SEM micrographs of clays being fired at 1280 °C

#### 4.3 Deterioration of samples by autoclave and bury technique

The clay samples were selected from previous part and the samples were tested by autoclave and bury technique. Chemically the clay mineral was composed basically of silicates, hydrous aluminum, iron and magnesium, which could be dispersed in fine particles. Presence of impurities such as ferric oxides, quartz among others played an important role on the characteristics of the final product. The chemical compositions of all samples were analyzed by X-Ray Fluorescence analysis in Table 4.7. Chemical composition of the fired JQA clay before autoclave and bury test were compared with the samples after test found that SiO<sub>2</sub> tended to decrease about 2.39 % after autoclave test. In the same way, SiO<sub>2</sub> composition was decreased about 2.25 % after bury test.



 Table 4.7 Chemical composition of samples

Samples	JQA.SH	JQA	JQA	JQA
		Samples	Autoclave	Bury
SiO <sub>2</sub>	76.69	87.51	85.12	85.26
Al <sub>2</sub> O <sub>3</sub>	10.82	10.33	11.85	6.91
K <sub>2</sub> O	2.62	0.67	0.44	1.05
Fe <sub>2</sub> O <sub>3</sub>	6.97	1.46	2.08	4.78
CaO	1.00	0.01		0.52
MnO	3/-	N-X	1 3	0.16
TiO <sub>2</sub>	1.72	0.01	0.50	1.15
$ZrO_2$	0.20	0.01	ERSI	0.13
LOI		4.07	_	

Copyright<sup>©</sup> by Chiang Mai University All rights reserved

Table 4.8 Autoclave test weight of drying mass

Weight of drying mass						
	Autoclave test					
	Weight (g)					
Initial	Autoclave	Mass loss				
47.0486	47.0372	0.0114				
47.8932	47.8724	0.0208				
47.3893	47.3505	0.0388				
	Initial 47.0486 47.8932	Autoclave test Weight (g) Initial Autoclave  47.0486 47.0372 47.8932 47.8724				

Table 4.8 shows drying weight comparison of the fired JQA sample before and after autoclave test. It was seen that mass loss was about 0.0114 g, 0.0208 and 0.0388 after autoclave for 6, 12 and 18 hours, respectively. The mass loss increased with longer autoclave time.

ลิขสิทธิ์มหาวิทยาลัยเชียงใหม่ Copyright<sup>©</sup> by Chiang Mai University All rights reserved

Table 4.9 Bury test weight of drying mass

	Weight of drying mass						
Samples Bury test							
Time (h)	Weight (g)						
	Initial	Bury	Mass loss				
90	47.4337	47.4315	0.0022				
180	47.7151	47.7094	0.0057				
360	47.9845	47.9683	0.0081				

Table 4.9 shows drying weight comparison of the fired JQA sample before and after buried test. It was found that mass loss was about 0.0114 g, 0.0208 and 0.0388 after autoclave for 90, 180 and 360 days, respectively. Similarly, to bury test, mass was slightly decreased with longer time, Table 4.9. The maximum loss was obtained after longer bury time.

Figure 4.24, 4.25 show SEM micrographs of fired JQA clays after autoclave at different times. After being autoclaved with different time, high densification of sample found that porous tended to increase when the time for test was increased in the range of 6, 12 and 18 hours. It was observed that the porosity was increased with increasing time in the process. It was due to the deterioration of glassy phase SiO<sub>2</sub> in ceramic matrix. Therefore, it was confirmed the previous results that SiO<sub>2</sub> can be removed from clay body due to the constant pressure during autoclave process. Moreover, glassy phase loss tended to increase when the holding time was increased.

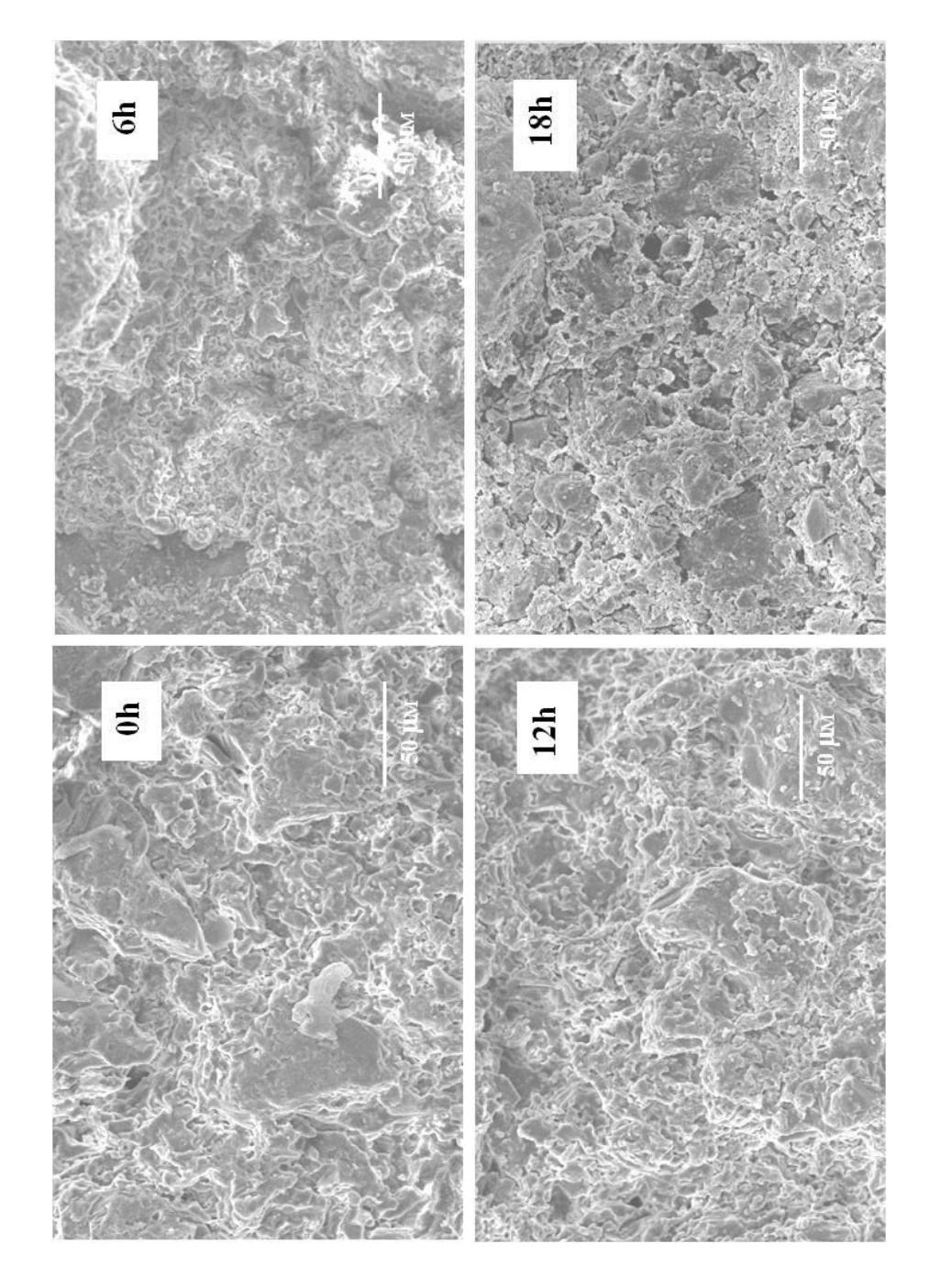


Figure 4.23 SEM of fired clays at different time for autoclave process 500x

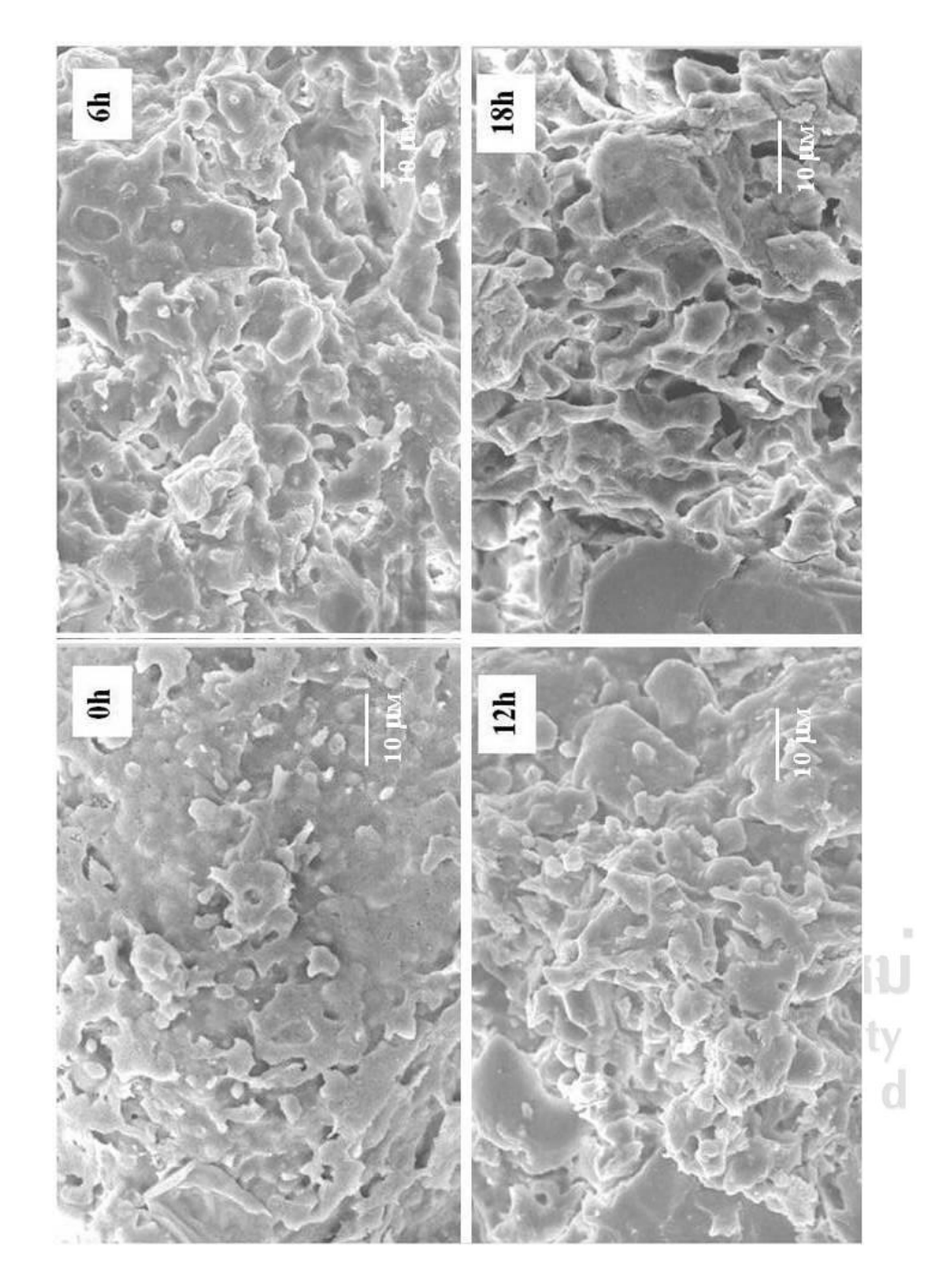


Figure 4.24 SEM of fired clays at different time for autoclave process1500x

Bury test was another process, which could prove the hypothesis about the degradation of ceramic. This process simulated the behavior of ceramic pottery, when it was buried in the soil. After buried at different times, the microstructure structure of samples was analyzed by SEM technique. SEM micrographs in Figure 4.25, 4.26 showed the relation of mass loss from samples with the different time. Higher porosity was observed which depended on the increasing time in bury process.

In the previous part, the research was clearly found out about the degradation of fired ceramic. It could be confirmed that fired ceramic degradation occurred under pressure and heat. That affected directly to pores and cracks defect in the structure of fired clay.



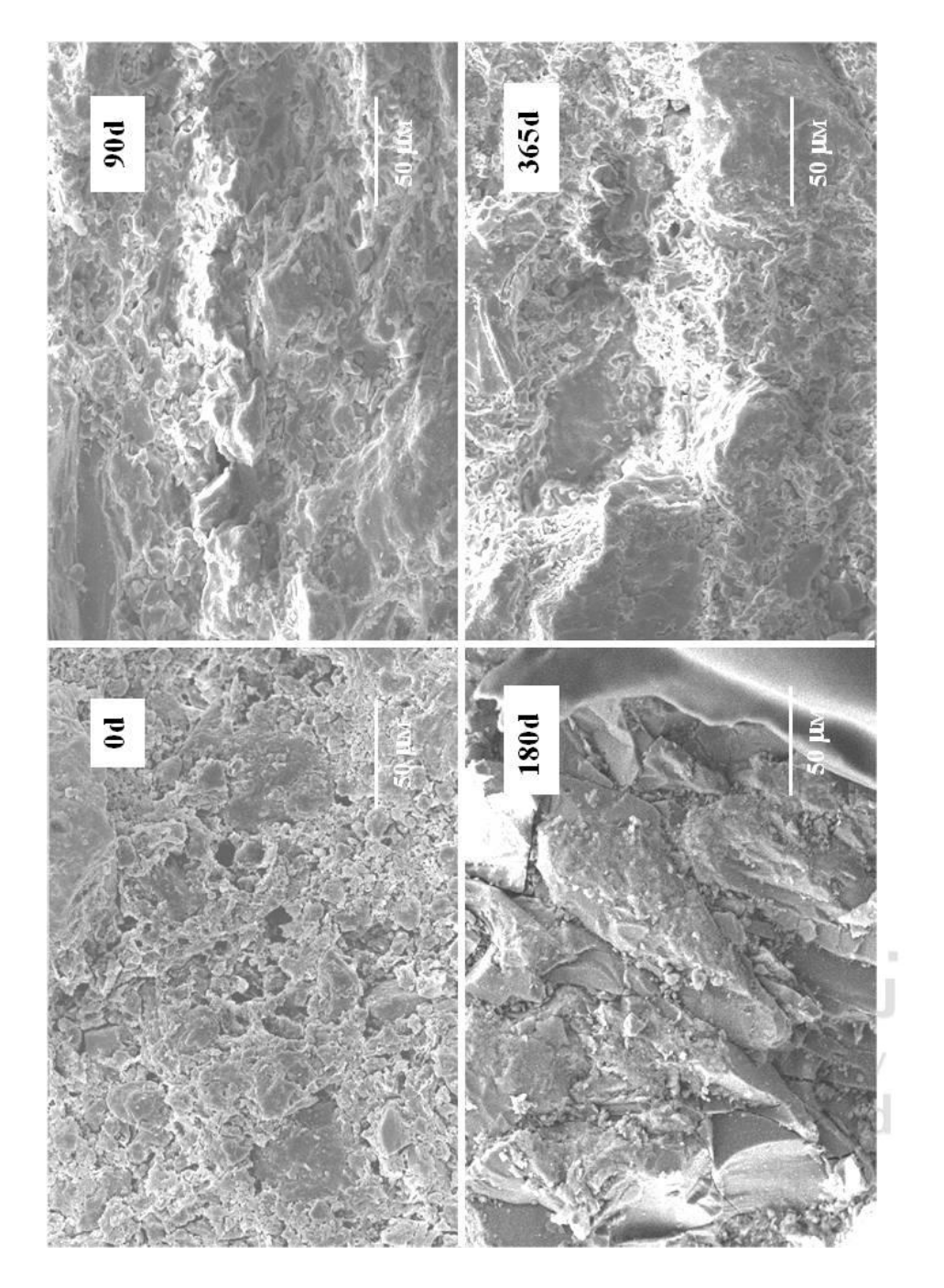


Figure 4.25 SEM of fired clays at different time for bury process 500x

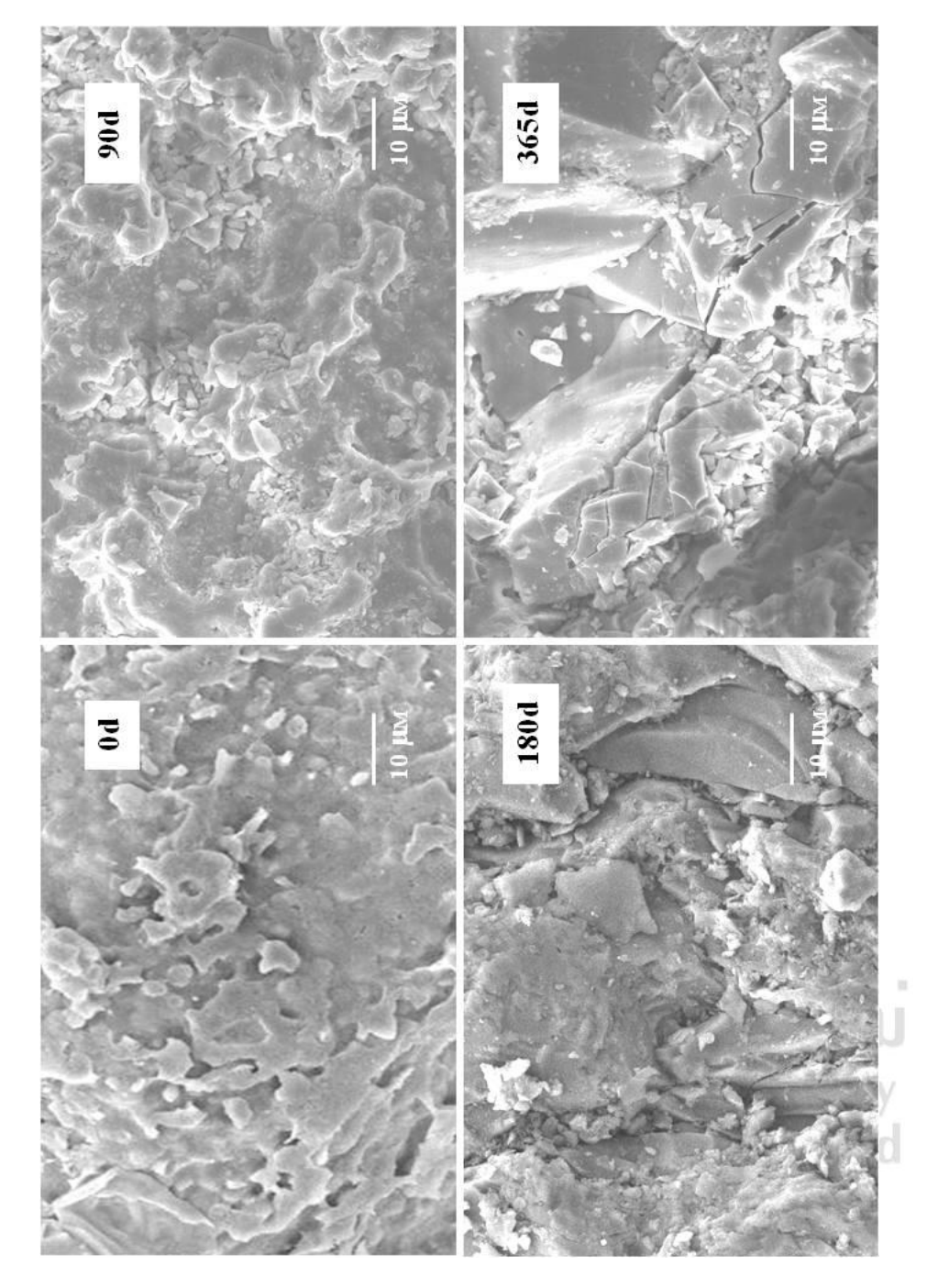


Figure 4.26 SEM of fired clays at different time for bury process 1500x